LAWRENCE
LIVERMORE
NATIONAL
LABORATORY

LLNL-PROC-655182

MACS: A high-efficiency, gated spectrometer for x-ray Thomson scattering on the National Ignition Facilitya

T. Doeppner, A. L. Kritcher, P. Neumayer, D. Kraus, B. Bachmann, S. Burns, R. W. Falcone, S. H. Glenzer, J. Hawreliak, A. House, O. L. Landen, S. LePape, T. Ma, A. Pak, D. Swift

June 2, 2014

20th Topical Conference on High-Temperature Plasma Diagnostics
Atlanta, GA, United States
June 1, 2014 through June 5, 2014

Disclaimer

This document was prepared as an account of work sponsored by an agency of the United States government. Neither the United States government nor Lawrence Livermore National Security, LLC, nor any of their employees makes any warranty, expressed or implied, or assumes any legal liability or responsibility for the accuracy, completeness, or usefulness of any information, apparatus, product, or process disclosed, or represents that its use would not infringe privately owned rights. Reference herein to any specific commercial product, process, or service by trade name, trademark, manufacturer, or otherwise does not necessarily constitute or imply its endorsement, recommendation, or favoring by the United States government or Lawrence Livermore National Security, LLC. The views and opinions of authors expressed herein do not necessarily state or reflect those of the United States government or Lawrence Livermore National Security, LLC, and shall not be used for advertising or product endorsement purposes.

MACS: A high-efficiency, gated spectrometer for x-ray Thomson scattering on the National Ignition Facility[a)]

T. Döppner,[1] A.L. Kritcher,[1] P. Neumayer,[2] D. Kraus,[3] B. Bachmann,[1] S. Burns,[1] R.W. Falcone,[3,4] S.H Glenzer,[5] J. Hawreliak,[1] A. House,[1] O.L. Landen,[1] S. LePape,[1] T. Ma,[1] A. Pak,[1] and D. Swift[1]

[1)] *Lawrence Livermore National Laboratory, Livermore, USA*
[2)] *Gesellschaft für Schwerionenphysik, Darmstadt, Germany*
[3)] *University of California, Berkeley, USA*
[4)] *Lawrence Berkeley National Laboratory, Berkeley, CA 94720, USA*
[5)] *SLAC National Accelerator Laboratory, Menlo Park, USA*

(Dated: 28 May 2014)

We have designed, built and successfully fielded a highly-efficient and gated Mono Angle Crystal Spectrometer (MACS) for x-ray Thomson scattering (XRTS) measurements on the National Ignition Facility (NIF). It utilizes a curved Bragg crystal based on Highly Oriented Pyrolytic Graphite (HOPG). Its spectral range of 7.4-10 keV is optimized for scattering experiments using a Zn He-α x-ray probe at 9.0 keV or Mo line emission around 18 keV in second diffraction order. The spectrometer has been designed as a DIM-based instrument for the NIF target chamber at the Lawrence Livermore National Laboratory, USA. Here we report on details of the spectrometer snout, its novel debris shield configuration and an in-situ spectral calibration experiment with a Brass foil target.

I. INTRODUCTION

Accurate characterization of warm and hot dense matter is important for high energy density physics experiments that aim at advancing our understanding of, for example, inertial confinement fusion [1,2] and astrophysical objects[3]. For example, the capability to measure electron temperature and density in dense matter provides key observables that allow validation of radiation hydrodynamic codes. X–ray Thomson scattering (XRTS) has been developed to accurately measure these plasma parameters at and above solid density in a series of experiments on the Omega laser at the Laboratory for Laser Energetics in Rochester, NY.[4] While most experiments used directly-driven planar foils[5], first experiments demonstrated XRTS from spherical shell targets[2] that took advantage of convergence effects to demonstrate characterization of electron densities as high as $n_e = 2 \times 10^{24}$ cm^{-3} with x-ray Thomson scattering[2].

Within the fundamental science program at the National Ignition Facility (NIF) at the Lawrence Livermore National Laboratory (LLNL) a series of equation-of-state (EOS) experiments was proposed to explore matter at extreme pressures that approach and exceed 1 Gbar[6], and to utilize XRTS as a temperature diagnostic at these extreme conditions. At sufficiently large x-ray photon energies and scattering angles XRTS is probing the response of individual electrons, and the shape of the inelastically down-scattered Compton profile reflects their velocity distribution in the plasma.[4] At the densities expected in these EOS experiments the plasma conditions become degenerate when the temperature exceeds 100 eV, and the width of the Compton profile allows to inferring the electron temperature. Details of the experimental platform including the scattering geometry[7] and additional design consideration[8] are reported elsewhere. Here we focus on the details of the XRTS spectrometer and its performance qualification.

A. MACS Spectrometer Design

It turns out, that the Zn He-α x-ray line at 9.0 keV is sufficiently high in photon energy to propagate through $\approx$ 1 mm of 4x compressed CH plastic as created in the NIF Gbar EOS experiments, for further details cf. Ref.[8]. Therefore, the design of the Mono Angle Crystal Spectrometer (MACS) is based on successful measurements with the Zn Spectrometer ZSPEC at the Omega laser.[5]. Fig. 1 shows details of the spectrometer design. In order to achieve high collection efficiency we use (i) highly oriented pyrolytic graphite (HOPG) as the Bragg crystal, which has the highest known integrated reflectivity on order of 5 mrad at 9 keV[9–11], and (ii) use a curved crystal in a von–Hámos type geometry[12] that focuses the x-ray signal in the non-dispersive direction. An additional feature of this geometry combined with proper shielding at the target is the ability to spatially discriminating undesired background signals[7]. The geometrical dimensions are determined by the constraints imposed by the dimensions of the NIF diagnostic instrument manipulators (DIMs) and the necessity to avoid interference with the NIF beams assuming the snout will be fielded in the polar DIM, and at the same time moving the crystal as far away from the aim point as possible to improve spectral resolution. As a result, we are using a 30 mm wide by 70 mm long HOPG crystal that has a radius of curvature (ROC) of 54 mm. As the energy that is reflected from the center

[a)] Contributed paper published as part of the Proceedings of the 20th Topical Conference on High-Temperature Plasma Diagnostics, Atlanta, Georgia, June, 2014.

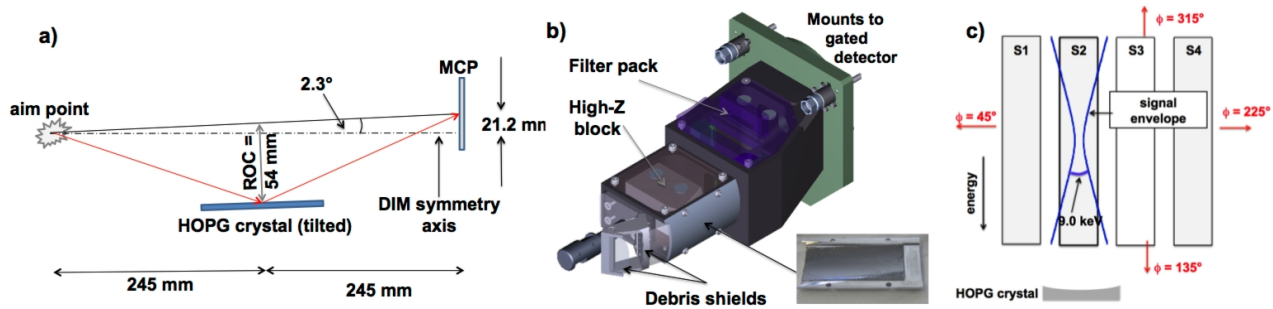

FIG. 1. a) Schematic geometry of Mono-Angle Crystal Spectrometer (MACS). b) CAD model of the MACS snout with one side removed to make the 20 mm HeavyMet shield visible. c) Simulated spatial signal envelope of x-rays focused to strip 2 of a 4-strip gated MCP detector as viewed from the back side of the snout with azimuthal chamber coordinates indicated.

of the crystal as shown in Fig. 1a we chose 8.6 keV. To satisfy the Bragg condition

$$n\lambda = n\frac{hc}{E_o} = 2d\sin\theta_B, \tag{1}$$

where n is the diffraction order, h is Planck's constant, c is the speed of light, λ is the x-ray wavelength, and $2d =$ 0.67 nm the HOPG lattice spacing, the corresponding central Bragg angle θ_B is 12.4°. In order fulfill the mosaic focussing condition for best spectral resolution (source to crystal equals crystal to detector), the distance from source to the center of the crystal is 251 mm, and the direct distance from the source to the detector to be 490 mm. The crystal substrate is made out of aluminum, and was machined at LLNL with high quality surface finish to the described curvature. A 300 μm thick HOPG coating layer was applied by Optigraph (Berlin). The mosaicity of the crystal is quoted to meet $\gamma \leq 0.8°$. The dispersion follows directly from the geometry[11], and is calculated to be 76 eV/ mm at 8.6 keV.

To avoid interference with neighboring NIF beams the symmetry axis of the spectrometer is tilted by 2.3° with respect to the DIM axis, reducing the crystal stand–off to 10.0° . Therefore, in order to correctly align the spectrometer, the whole DIM cart holding the gated detector needs to be offset by 21.2 mm from the DIM symmetry axis. The alignment is controlled by standard alignment fiducials in the front of the snout (cf. Fig 1a). The front edge of this feature is aligned at 130.3 mm from the aim point. A new debris shield configuration was developed and tested for this particular which is unique from other snouts in that it has a large open aperture on order of 30 mm x 15 mm. We are fielding a 25 um (??) thin Kapton pre-filter at an angle of x ° with respect to the central x-rays, which is tasked to absorb the soft x-ray load. This pre-filter is tilted such that its normal does not intersect the main front filter. The main blast shield is built out of 700 um polycarbonate, and is supported by a line array of 2 mm wide aluminum bars. The blast shield support structure, shadowing some parts of the HOPG crystal, reduces its effective width to ca. 22 (??)mm. The angle between the the normal of the polycarbonate foil and the central x-ray beams is 22.5°, increasing its effective thickness to 758 μm. Another feature of this snout is the ca. 40 mm thick tantalum block to shield the detector from super hard x-rays (> 50 keV) generated by laser plasma interactions in the hohlraum[13].

II. MACS CALIBRATION EXPERIMENT N130322

For performance qualification we have completed a calibration experiment inside the NIF target chamber (shot N130322-001-999). For this purpose we irradiated a 3 mm square, 12 μm thick brass foil (alloy consisting of 68.5-71.5% Cu, 28.4-31.1%, < 0.1% Pb and Fe) with a 15 TW 1 ns-square pulse produced by 2 quads, Q46T and Q46B. Taking incident angles into account, the standard phase plates produced an elliptical spot size of 1.10 mm × 0.83 mm, which yielded an intensity of 2.1×10^{16} W/cm^2. The spectrometer has a direct view of the driven side of the brass foil, which is vertical in the target chamber with its normal aligned along the dispersion axis of the spectrometer ($\phi = 135°$) to minimize the apparent laser spot size to 145 um. For signal detection we use a four strip micro channel plate detector which is fiber optically coupled to a CCD. All strips were co-timed with the center of the strip at 0.62 ns after the start of the laser drive. The integration time is 100 ps, and the strip transit time is 200 ps with the high energy (10 keV) x-rays recorded later than the lower energy side of the spectrum (7.5 keV). To reduce the photon flux at the detector, we added 889 μm aluminum in addition to the standard plastic filtering. Fig. 2 shows the raw data recorded by the MACS spectrometer on N130322. One can clearly observe line emission from Cu and Zn K-shell transitions on top of a continuum background. The latter is from thermal emission in second diffraction order which becomes comparable to the line emission due to the strong Al filtering (9.5×10^{-5} transmission at 8.6 keV). The second order continuum also shows the typical spatial defocusing away from the center energy which is due to the detector position vertical to the symmetry axis. At 8.6 keV the x-rays are collimated to a best focus of 2.7 mm. Assum-

ing 1.1 mm spot size in the non-dispersive direction, and considering that the focal spot size increase with HOPG mosaicity γ as $d_{foc} = 2ROC \tan\gamma$, one can infer the mosaicity to be $\gamma = 1.3°$. This is larger than specified by the supplier, possibly due to the fact that the ≈17 keV x-rays probe rather deep layers in the HOPG crystal. To extract the calibration spectrum in first diffraction order we integrated the full signal, taken into account the curvature of iso-energy contours as apparent for the Cu He-β doublet, which is in agreement with our raytracing model. After subtracting the second order continuum, we corrected the spectrum with respect to the filter transmission (889 μm Al, 772 μm Polycarbonate, 300 μm Kapton), and for the change in dispersion and collection angle as function of energy. The resulting spectrum is shown in Fig. 3. The most prominent lines are the Cu He-α (8.347 & 8.392 keV) and Zn He-α (8.950 & 8.999 keV) lines along with a pronounced doublet at 9.75 keV which is assigned to Cu He-β (9.862 & 9.875 keV) and a Li-like intercombination line (9.748 keV). At the high energy edge of the spectrum appears to be Li-like intercombination line (10.223 keV) of Cu He-γ. The 1-3 transitions can be used to infer the spectral resolution.

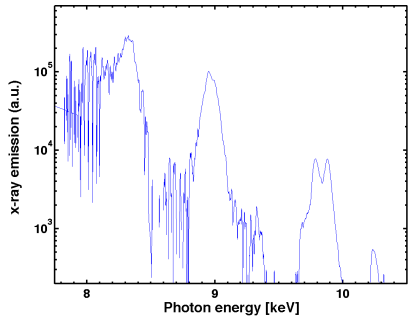

FIG. 3. Brass foil spectrum, intensity corrected for filter transmission and other effects.

ACKNOWLEDGMENTS

We acknowledge help from Dan Kalantar, Tom McCarvillle and Reg Wood who worked out critically important alignment procedures. We also would like to thank Ulf Zastrau and Vladimir Arkadiev for helpful discussions on graphite coatings. Sean Felker for technical support building the Brass foil target. This work was performed under the auspices of the U.S. Department of Energy by the Lawrence Livermore National Laboratory, through the Institute for Laser Science and Applications, under contract DE-AC52-07NA27344. The authors acknowledge support from Laboratory Directed Research and Development Grant No. 13-ERD-073.

[1] J. D. Lindl, P. Amendt, R. L. Berger, S. G. Glendinning, S. H. Glenzer, S. W. Haan, R. L. Kauffman, O. L. Landen, and L. J. Suter, Phys. Plasmas **11**, 339 (2004).

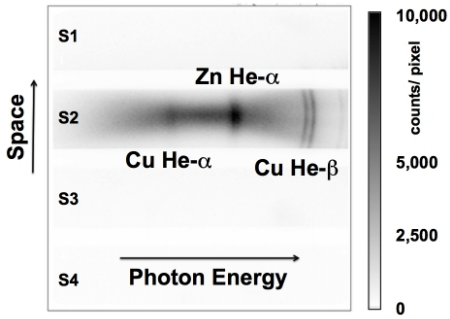

FIG. 2. Raw experimental data recorded at the performance qualification experiment N130322.

[2] A. L. Kritcher, T. Doeppner, C. Fortmann, T. Ma, O. L. Landen, R. Wallace, and S. H. Glenzer, PHYSICAL REVIEW LETTERS **107** (2011).
[3] L. Stixrude, PHYSICAL REVIEW LETTERS **108**, 055505 (2012).
[4] S. Glenzer and R. Redmer, Rev. Mod. Phys. **81**, 1625 (2009).
[5] T. Ma, T. Doppner, R. W. Falcone, L. Fletcher, C. Fortmann, D. O. Gericke, O. L. Landen, H. J. Lee, A. Pak, J. Vorberger, K. Wünsch, and S. H. Glenzer, PHYSICAL REVIEW LETTERS **110**, 065001 (2013).
[6] A. L. Kritcher, T. Döppner, D. Swift, J. Hawreliak, G. Collins, J. Nilsen, B. Bachmann, E. Dewald, D. Strozzi, S. Felker, O. L. Landen, O. Jones, C. Thomas, J. Hammer, C. Keane, H. J. Lee, S. H. Glenzer, S. Rothman, D. Chapman, D. Kraus, P. Neumayer, and R. W. Falcone, HIGH ENERGY DENSITY PHYSICS **10**, 27 (2014).
[7] T. Döppner, A. Kritcher, S. Glenzer, B. Bachmann, D. Chapman, G. Collins, R. Falcone, J. Hawreliak, D. Kraus, O. Landen, H. Lee, S. L. Pape, T. Ma, P. Neumayer, R. Redmer, and D. Swift, accepted for publication in J. Phys.: Conf. Series (2014).
[8] D. Chapman, T. Doeppner, A. L. Kritcher, D. Kraus, B. Bachmann, L. O. L, S. H. Glenzer, D. C. Swift, and H. J, submitted to Physics of Plasmas (2014).
[9] B. Beckhoff, B. Kanngiesser, and W. Malzer (SPIE, 1996) pp. 190–199.
[10] T. Döppner, P. Neumayer, F. Girard, N. Kugland, O. Landen, C. Niemann, and S. Glenzer, Rev. Sci. Instrum. **79**, 10E311 (2008).
[11] A. Pak, G. Gregori, J. Knight, K. Campbell, D. Price, B. Hammel, O. L. Landen, and S. H. Glenzer, Review of Scientific Instruments **75**, 3747 (2004).
[12] L. von Hamos, Ann. Phys. **17**, 716 (1933).
[13] T. Doeppner, C. A. Thomas, L. Divol, E. L. Dewald, P. M. Celliers, D. K. Bradley, D. A. Callahan, S. N. Dixit, J. A. Harte, S. M. Glenn, S. W. Haan, N. Izumi, G. A. Kyrala, G. LaCaille, J. K. Kline, W. L. Kruer, T. Ma, A. J. MacKinnon, J. M. McNaney, N. B. Meezan, H. F. Robey, J. D. Salmonson, L. J. Suter, G. B. Zimmerman, M. J. Edwards, B. J. MacGowan, J. D. Kilkenny, J. D. Lindl, B. M. Van Wonterghem, L. J. Atherton, E. I. Moses, S. H. Glenzer, and O. L. Landen, PHYSICAL REVIEW LETTERS **108** (2012).